

Influence of cellulose acetate polymer proportion on the fabrication of polyvinylchloride reverse osmosis blend membrane, experimental design

Heba Abdallah^{a,*}, Ayman El Gendi^{a,b}, Marwa S. Shalaby^a, Ashraf Amin^a, Mahmoud El- Bayoumi^c, A.M. Shaban^d

^aChemical Engineering and Pilot Plant Department, Eng. Research Division, National Research Centre, Dokki, Giza, Egypt, email: heba_nasr94@yahoo.com, drhebaabdallah3@gmail.com (H. Abdallah)

marwashalaby14@gmail.com (M.S. Shalaby), ashmukhtar@yahoo.com (A. Amin)

^bDepartment of Chemical and Materials Engineering, Faculty of Engineering, King Abdulaziz University, Jeddah, Kingdom of Saudi Arabia, email: aymentaha2010@yahoo.com, aelgendi@kau.edu.sa (A. El Gendi^a)

^cMechanical Engineering Department, Engineering Research Division, National Research Centre, email: el_bayoumi@hotmail.com (M. El- Bayoumi)

^dWater Pollution Research Department, Environmental Research Division, National Research Centre, 33 El-Bohouth St. (Former El-Tahrir St.), Dokki, Giza, Egypt, PO box 12622, Affiliation ID: 60014618, Tel. +202 33335494, Fax +202 33370931, email: ashaban12311@gmail.com (A.M. Shaban)

Received 20 November 2017; Accepted 4 April 2018

ABSTRACT

The current research aims at introducing polyvinylchloride (PVC) favorable properties such as strength, durability, and low cost to RO membranes through blending it with cellulose acetate (CA). Hence, blend membranes of PVC/CA have been prepared and developed for water desalination. Large-scale membranes (110 cm long × 65 cm wide) were fabricated using a homemade batch casting machine. To save chemicals cost, reduce experimental errors and reduce the number of experiments, a factorial design employing response surface methodology (FDRSM) has been established using experiment design software. Produced PVC/CA membranes were characterized using Scanning electron microscopy (SEM), Thermo gravimetric analysis (TGA) and tensile testing. The performance of prepared PVC/CA membranes has been examined using a homemade lab-scale desalination-testing unit to study salt rejection and water permeate flux. The results established that a PVC/CA blended membrane with 14% PVC and 2% CA, at 30 bars of pressure, achieves salt rejection of 99%, 99.2% and 99.6% from feeds with salt concentrations of 45000, 18000 and 5000 ppm respectively.

Keywords: Polyvinylchloride, Cellulose acetate, Membrane fabrication, Desalination

1. Introduction

Lately, membrane separation technology is getting higher penetration into engineering applications of filtration and separation of liquid streams and gaseous mixtures. Membranes excelled in treatment of industrial effluents [1–5]. In food and drug industries, ultrafiltration (UF) membranes are used to fractionate macromolecular solutions. In

medical applications they excel in removing toxins from the blood stream by dialysis [6–8].

Reverse osmosis (RO) technology employs a semipermeable membrane to separate ions, molecules, and very tiny particles from water. An applied pressure is used to overcome osmotic pressure, where the solute is retained on the pressurized side of the membrane and the treated water passes to the other side [4–9]. Recently, RO membranes are used to produce drinking water from seawater, wells, and groundwater via desalination [1–3].

*Corresponding author.

The most common polymeric membrane preparation process is phase inversion process, where a polymer is dissolved in an appropriate solvent and is cast using a film applicator on a substrate such as glass or Teflon. The cast membrane is immersed in a liquid bath as water for coagulation; during that a homogeneous polymer membrane is formed. The formed membrane contains a network of uniform pores [3,9,10]. This process allows for polymer blending.

Polymer blending can lead to improving membranes by combining the properties of the mixed polymers, such as hydrophilicity, hydrophobicity, performance, and rejection percentage [11–13]. By blending PES with cellulose acetate (CA), improved membranes were produced with salt rejection of 99% and permeate flux of 21 kg/m²·h for 6000 ppm salty water concentration [14,15]. Addition of metal organic compound such as Mn(acac)³ in the polymer solution mixture of polyethersulfone led to improving the hydrophilicity of the prepared membrane [11]. Blending PES polymer with titanium dioxide nanotubes also can improve membrane hydrophilicity, then membrane performance, where the rejection percentage reached to 99% with a permeate flux of 18.2 kg/m²·h for 8000 ppm salty water [13]. Also, the selection of appropriate solvent is a significant factor for successful blending of polymeric solutions [11].

Actually, the membrane separation technology has proved faster, more efficient, and more economical than traditional separation techniques [1–5]. However, lowering the cost increasing durability and performance of membranes will allow better chances for its application.

The objective of this work is to investigate blending of cellulose acetate (CA) and polyvinylchloride (PVC) to produce low cost, durable large scale RO membranes that can be used in production of spiral wound modules. In this study, the effect of blending ratios between the two polymers was investigated. In first stage experimental design software was employed to arrange the experiments and facilitate exploring the optimum conditions. In the second stage, the blended membranes were prepared. In third stage, the membranes were characterized using SEM, TGA, BET area and tensile testing. In last stage, the performance of the prepared membranes was investigated using a desalination-testing unit.

2. Materials and methods

2.1. Materials

Analytical grade N-methylpyrrolidone (NMP) solvent, polyvinylchloride and cellulose acetate polymers were supplied by Sigma-Aldrich. Fluka supplied polyethylene glycol (PEG 400), which was used as a plasticizer.

2.2. Design of membrane preparation experiments using factorial design software

A factorial design with response surface methodology (FDRSM) using Design Expert software version (8.0) has been adopted to decrease the number of membrane preparation experiments. The factorial design helped to determine optimum percentage of polymers to fabricate higher

performance of RO blend membranes. Performance was evaluated based on salt rejection percentage and permeate flux. For the study, Polyvinylchloride (PVC), denoted as A, and Cellulose Acetate (CA), denoted as B, were blended.

2.3. Fabrication of PVC/CA blend membranes

Large-scale PVC/CA blend membranes were prepared using a homemade batch-casting machine. The casting machine was designed and fabricated in our lab. It produces membrane sheets of up to 110 cm length and 65 cm width. Fig. 1 shows the batch-casting machine. The machine was designed to prepare phase inversion membranes induced by immersion precipitation method within the machine.

Experiments showed that mixing speeds higher than 400 rpm increases the air bubbles inside the polymeric solution due to its high viscosity. Accordingly, for the current study, the agitation speed was fixed at 400 rpm for all polymer solution preparations. The prepared casting solution of PVC/CA in NMP was cast onto a glass plate. The glass plate was immersed in pure water. After membrane coagulation, the membrane was stored in another fresh water bath for 24 h to guarantee complete phase inversion and to ensure complete removal of solvent residuals [3–6].

By varying PVC/CA concentrations, different RO membrane grades were produced. Table 1 displays the compositions, which were used to prepare PVC/CA blend membranes. In order to minimize the experimental errors



Fig. 1. Batch casting machine.

Table 1
Polymer blend solutions composition

Membrane type	PVC %	CA%	PEG%	NMP%
M 1	16	2	1	81
M 2	16	1	1	82
M 3	15	1	1	83
M 4	14	3	1	82
M 5	14	2	1	83

each type of membranes has been prepared at least three times, to ensure repeatability of properties.

2.4. Membrane characterization

2.4.1. Scanning electron microscopy (SEM)

Scanning electron microscopy (SEM) has been used to investigate the morphology of PVC/CA membranes. The cross-sectional images of the membranes were taken using a JEOL 5410 scanning electron microscope (SEM). The test was conducted at a voltage of 20 kV.

2.4.2. Mechanical properties

Mechanical properties of PVC/CA blend membranes were studied to determine the effect of PVC and CA percentages on membrane strength. The tensile strength and elongation of the membranes were measured using mechanical testing system (INSTRON-5500R). The gauge length and width of dumbbell tensile specimens were 6.2 mm and 0.16 mm, respectively. The tensile strength and elongation have been measured several times (at least three times) in order to minimize experimental errors and the results have been reported as an average [12].

2.4.3. Membrane porosity and BET area

Porosity and inner surface area of prepared membranes were determined using the Brunauer-Emmett-Teller (BET) method. Samples of known weights of the membrane were cut into strips and placed in the glass column of the apparatus, dried and degassed by heating at 80°C for 3 h. The average area was determined using the BET single point technique. Also, the porosity of prepared blend membranes were determined.

2.4.4. Thermo gravimetric analysis (TGA) and differential scanning calorimetry (DSC)

The TGA was carried out using thermal analysis instrument SDT Q600 V20.9. Samples of 1.8 mg of the membrane of highest salt rejection and pure PVC membrane, for comparison, were heated from 30 to 350°C at a heating rate of 10°C/min under nitrogen atmosphere. The DSC measurements of all prepared membranes' samples were carried out using the same instrument at a heating rate of 10°C/min under nitrogen atmosphere.

2.5. Membrane performance measurements

The membrane performance experiments have been carried out using a homemade laboratory desalination-testing unit shown in Fig. 2. This system contains a stainless steel flat sheet membrane testing module that houses 11cm diameter membrane samples. The module is featured with three ports for feed (salty water), concentrate, and permeate. Membranes were tested for capacity of water separation at different salt concentrations of 5000, 18000 and 45,000 ppm. Synthetic salty water was continuously fed to the membrane testing module from a feeding

tank using a high-pressure pump. The product has been collected from permeate output to determine flux and rejection percentage.

The experimental water flux J_w (L/m² h) is given by the following equation [11]:

$$J_w = \frac{V}{A \cdot t} \quad (1)$$

where V is the volume of pure water permeate (L), A is the effective area of the membrane (m²), t is the permeation time (h).

The total dissolved solids (TDS) of the produced water were measured using a conductivity meter of model Adwa (AD 310), EC/temp meter is made in Romania. The salt rejection (R_f %) was conducted in triplicates for each membrane and the averages were calculated using the following equation [11]:

$$R_f \% = 1 - \frac{C_p}{C_f} * 100 \quad (2)$$

where C_f – feed bulk concentration (ppm); C_p – permeate concentration (ppm).

3. Results and discussions

3.1. Experimental design

The Factorial design and response surface methodology (FDRSM) are applied for phase inversion membrane preparation. FDRSM needs a selection of responses, factors, and levels. Salt rejection percentage and permeate flux (L/m²·h) responses were chosen to reflect the efficiency of membrane performance. The factors included in this study are mixing temperature, polymer (A) weight percentage, and polymer (B) weight percentage. The maximum and minimum levels for each factor were chosen as following, temperature (from 25 to 60°C), polymer A (PVC) weight percentage (from 0 to 20%), and polymer B (CA) weight percentage (from 0 to 20%). According to FDRSM analysis, 20 runs had to be

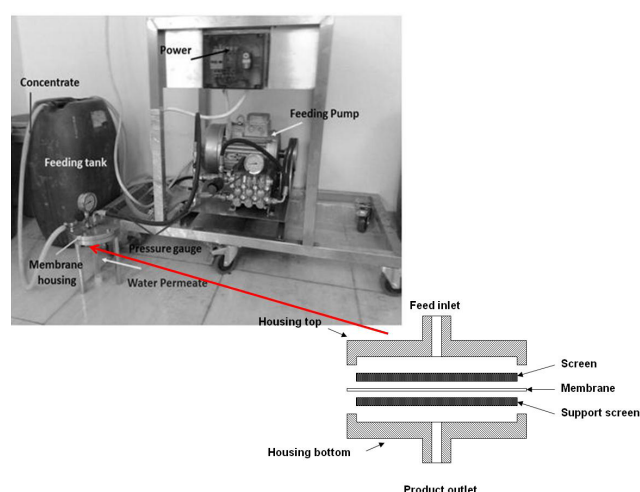


Fig. 2. Desalination testing unit and schematic diagram of the test chamber.

conducted using these operating conditions. The process factor coded model equation, for salt rejection percentage response can be calculated from the following equation (predicted by the software):

$$\text{SR}\% = 80 + 7.66A + 2.25B + 1.05C + 3.21A.C \quad (3)$$

$$+ 4.26A.B + 9.31B.C + 4.75A^2 + 5.8B^2 + 6.8C^2$$

where SR% is salt rejection percentage; A is PVC polymer percentage; B is CA polymer percentage; C is the temperature in Celsius degree.

Process factor coded model equation for permeate flux response ($\text{L}/\text{m}^2\cdot\text{h}$) can be calculated from the following equation (predicted by the software):

$$\text{Flux} = 89 + 8.5A + 4.14B + 1.06C + 5.42A.B + 6.12A.C \quad (4)$$

$$+ 3.22B.C + 5.82A^2 + 1.85B^2 + 8.43C^2$$

Figs. 3a and b show the contours and the three-dimensional response surface of salt rejection percentage as a function of polymers composition percentages (A and B) at the low-level temperature (25°C). FDRSM model predicted the salt rejection to be in the range of 85–95%. The model predicted that increases of polymer (A) weight percentage and decreases of polymer (B) weight percentage would lead to an increase in salt rejection percentage. Theoretically, increasing main polymer content would decrease the pores sizes, which would increase the salt rejection percentage [15].

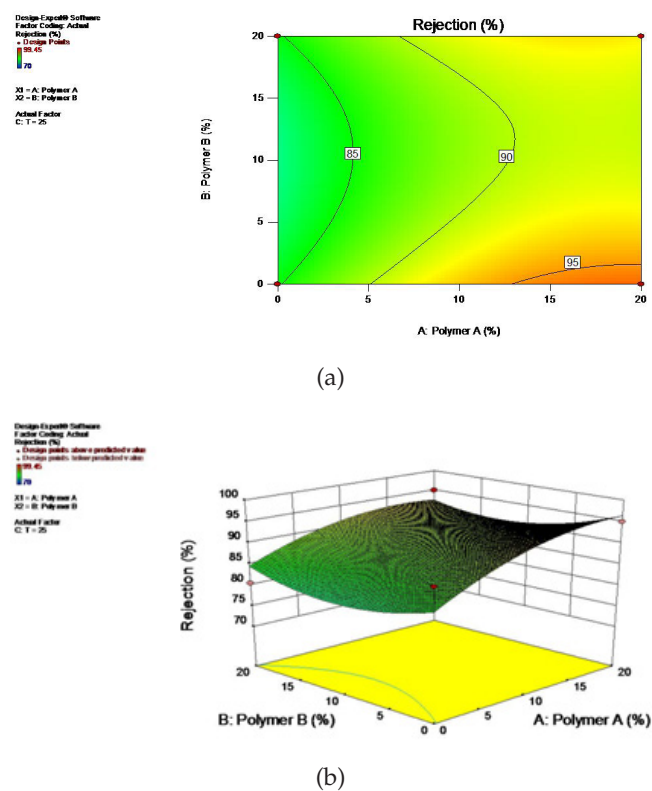


Fig. 3. FDRSM model solution of salt rejection percentage as function of polymer A and polymer B composition at 25°C , where (a) contour graph and (b) three dimension response surface plot.

Figs. 4a and b illustrate the predicted contours and the three-dimensional response surface of permeate flux as a function of the polymers composition percentages (A and B) at the low-level temperature (25°C). FDRSM model predicted permeate flux to be in the range of 90–110 $\text{L}/\text{m}^2\cdot\text{h}$. Increasing polymer (A) weight percentage and decreasing polymer (B) weight percentage would lead to a decrease in permeate flux. This, theoretically, is attributed to decrease in the membrane pores sizes, which would enhance the salt rejection percentage but would decrease the permeate flux [9,15].

Increasing polymer solution concentration causes thickness increase of the active dense layer, which lead to increase of salt rejection. Mainly, increasing of polymer concentrations in the casting solution lead to decrease membranes porosity, as a result of this slows down the de-mixing process, leads to a much higher polymer concentration at the interface [9,15,16], and increases the thickness of the top layer and decreases the porosity of the membrane.

Figs. 5a and b show the contour and the three-dimensional response surface for salt rejection percentage as a function of polymers composition (A and B) at the high-level temperature (60°C). FDRSM model predicted a salt rejection percentage in the range of 75–90%. Increasing polymer (A) weight percentage and decreasing polymer (B) weight percentage leads to an increase in salt rejection percentage. Increasing mixing temperature caused a drop in salt rejection percentage. The salt rejection percentage dropped from 95% to 90% by increasing the mixing tem-

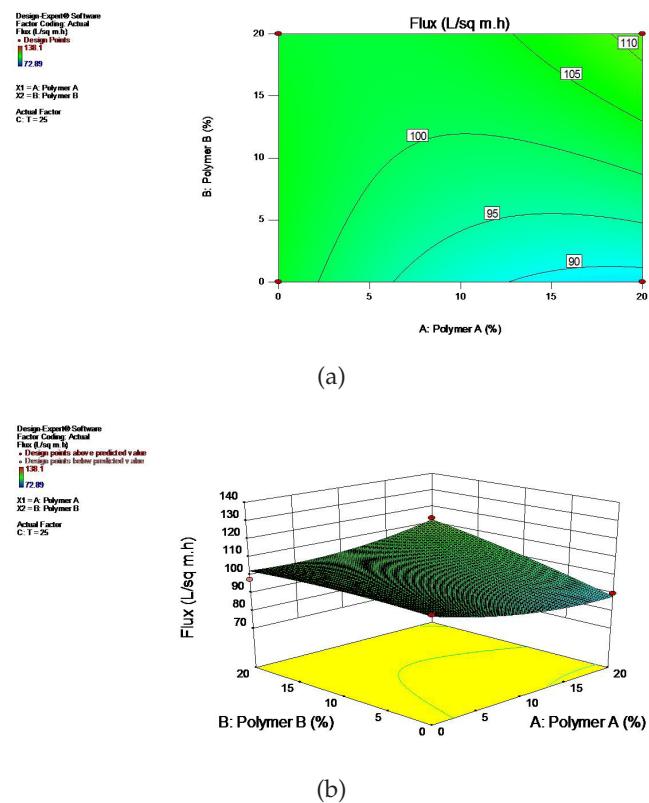


Fig. 4. FDRSM model solution of permeate flux as function of polymer A and polymer B composition at 25°C , where (a) contour graph and (b) three dimension response surface plot.

perature from 25 to 60°C. Increasing mixing temperature decreases the viscosity of the polymer solution leads to fast rate of coagulation during membrane casting [15,16], which in turn leads to decrease in membrane top layer thickness and, consequently, decreases salt rejection percentage.

Figs. 6a and b show the contour and the three-dimensional response surface of permeate flux as a function of polymers composition (A and B) at the high-level temperature (60°C). FDRSM model predicted that permeate flux would be in the range of 80–130 L/m².h. Increasing polymer (A) weight percentage and decreasing polymer (B) weight percentage would lead to a decrease in permeate flux, as discussed earlier, but improves salt rejection.

While increasing polymers mixing temperature from 25 to 60°C improved membrane flux and decreased salt rejection [16]. Increasing polymers content of A and B with a high temperature of the polymeric solution, leads to improvements in the permeate flux from 80L/m².h to 130 L/m².h but with a decrease in salt rejection, this may be due to voids and cracks can be formed in membranes after casting step according to mixing delayed for very high polymer content concentration [9,16]. Increasing polymers mixing temperature enhanced the membrane permeate while the salt rejection decreased, where increasing the main polymer (A) percentage and using low percentage of polymer (B) decreased the flux and improved the salt rejection, which was matched with the performance results due to increase in dense top layer thickness of formed membranes.

In our case, the polyvinyl chloride (PVC) has good mechanical strength, abrasion resistance, chemical stabilization, thermal properties, corrosion resistance and low cost. Using high percentage of PVC can produce hydrophobic membrane, while cellulose acetate (CA) membranes has moderate flux, high salt rejection, cost effectiveness, hydrophilic nature, and is non-toxic. On the other hand, cellulose acetate is not suitable for aggressive cleaning processes due to its low oxidation and chemical resistances, and its poor mechanical strength. By blending PVC with CA, prepared membranes would exhibit favorable properties of the two polymers and would have a very good performance. However, the presence of acetyl groups in cellulose acetate seems to influence the blended PVC/CA and causes produced membranes to be hydrophilic, which enhances anti-fouling properties and leads to improvement in permeate flux and salt rejection [17–20].

3.2. Membrane characterization

3.2.1. Scanning electron microscopy (SEM)

SEM images of prepared PVC/CA blend membranes are shown in Figs. 7–11. Fig. 7 shows the SEM image of the membrane M1 that was made of 16% PVC and 2% CA. The image shows a thin top dense layer and a spongy like structure with little finger like structures in the sub-layer. Fig. 8 illustrates the SEM image of the membrane M2 that was prepared using 16% PVC and 1% CA. The membrane has

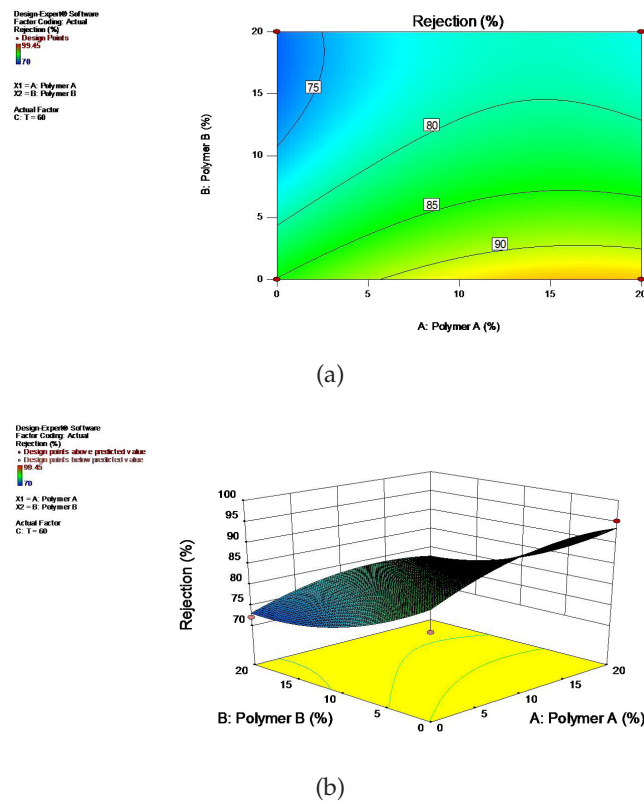


Fig. 5. FDRSM model solution of rejection percentage as function of polymer A and polymer B composition at 60°C, where (a) contour graph and (b) three dimension response surface plot.

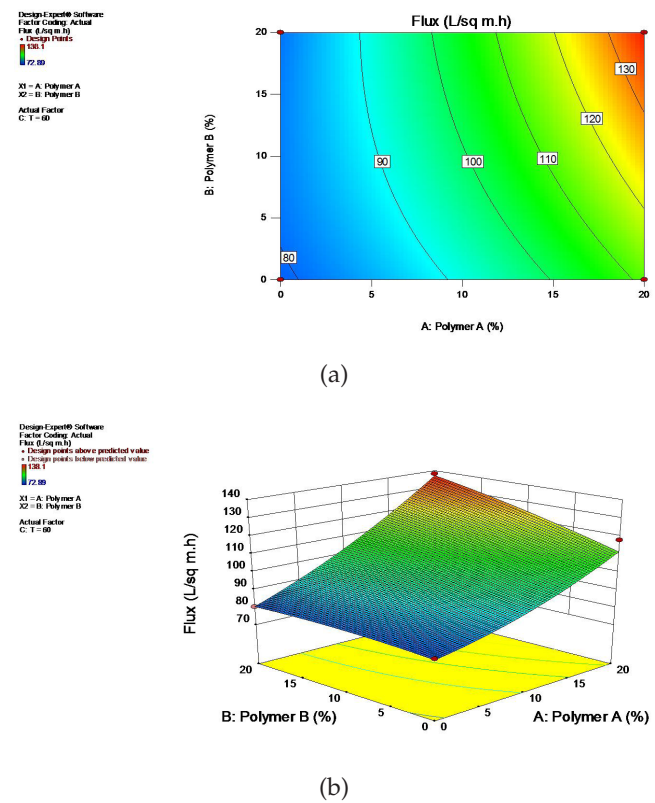


Fig. 6. FDRSM model solution of permeate flux as function of polymer A and polymer B composition at 60°C, where (a) contour graph and (b) three dimension response surface plot.

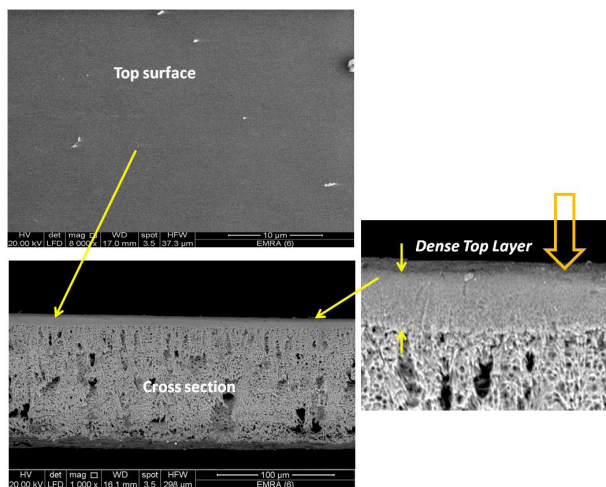


Fig. 7. SEM photos of prepared membrane (M1), thickness 230 μm .

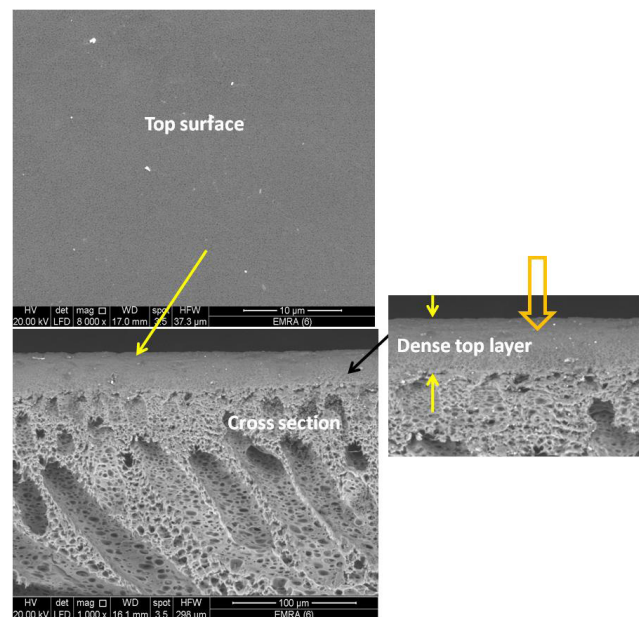


Fig. 10. SEM photos of prepared membrane (M4) thickness 109 μm .

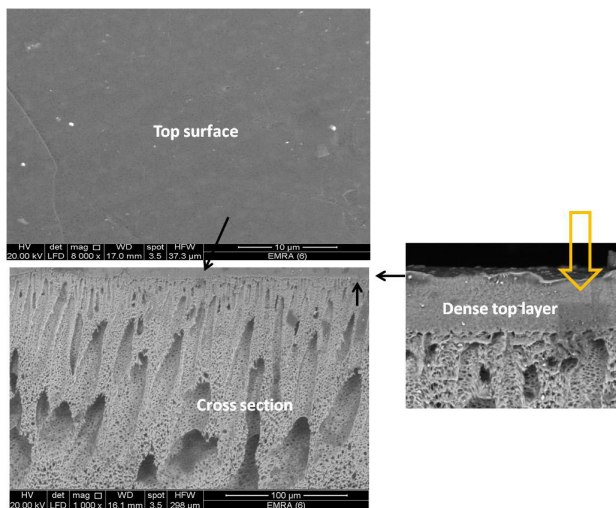


Fig. 8. SEM photos of prepared membrane (M2), thickness 200 μm .

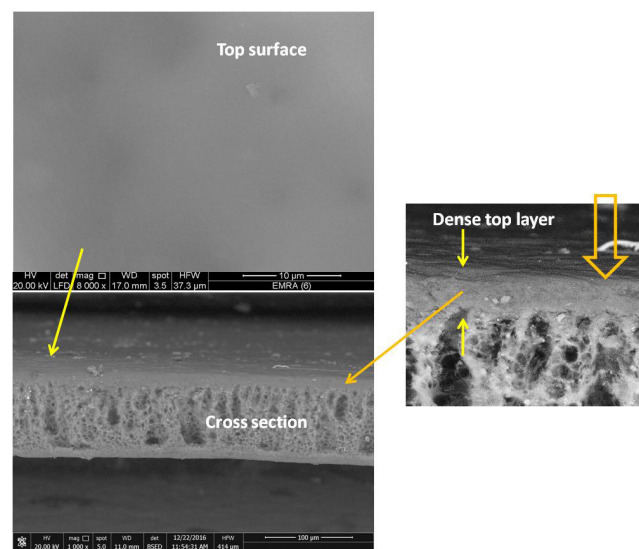


Fig. 11. SEM photo of prepared membrane (M5) thickness 150 μm .

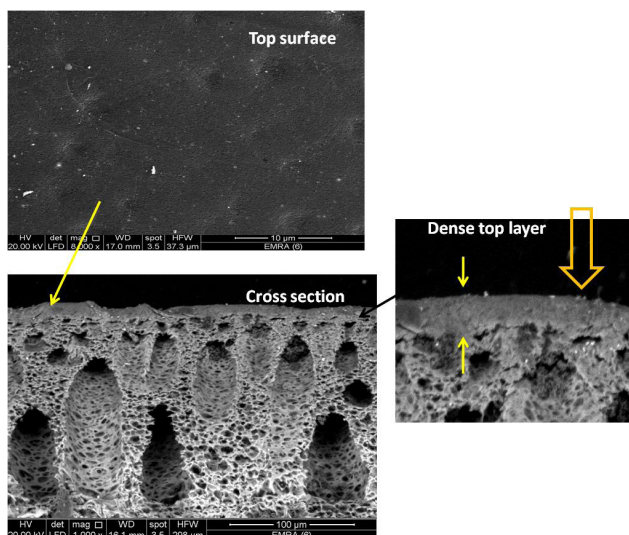


Fig. 9. SEM photos of prepared membrane (M3), thickness 90 μm .

finger-like pores with a thicker wall. The top dense layer of M2 is thinner than M1. The thinning of M2 dense layer is attributed to the decrease in CA weight percentage. During coagulation, the de-mixing of M2 was faster than M1. Fig. 7 and Fig. 8 indicate that the top dense layer is formed mostly from CA while the bottom layer is formed mostly from PVC [17–32].

Fig. 9 shows the SEM image of the membrane M3 that was prepared using 15% PVC blended with 1% CA. In this case, the dense top layer followed by large finger-like porous structure in sub-layer. The decrease of PVC percentage content to 15% increased the pore sizes of sub-layer, which would lead to improvement in the permeate flux.

Fig. 10 shows SEM image of the membrane M4 that was prepared using 14% PVC and 3% CA. The asymmetric membrane has fingers-like pores structure with a dense top layer, which indicates that the membrane can provide good permeate flux. During coagulation of M4, fast de-mixing has taken place in the coagulation bath. However, decreasing the PVC percentage to 14% and increasing CA percentage to 3% improved the asymmetric shape of the membrane structure and increased the dense layer thickness. M4 has a total polymer content of 17% compared to M3, which has less polymer content [16,19].

Fig. 11 shows the SEM image of the membrane M5 was prepared using 14% PVC and 2% CA. The membrane has asymmetric finger-like pores with a thick wall and dense top layer, which indicate that M5 can provide good permeate flux and good salt rejection percentage. The structure of M5 is attributed to rapid clustering of polymer segments into groups, which minimizes the polymer molecules interaction with non-solvent, [19–21].

The SEM images of the prepared PVC/CA membranes, as shown in Figs. (7–11), indicate that the structure of the membrane appears to be pore-free on the top (air side) but highly porous on the bottom (glass side) surfaces. The prepared membranes samples appeared to be asymmetric membranes, which mean that these membranes compose of numbers of layers each layer has different morphological structure like dense layer on the top surface, finger like structure in the middle layer and porous layer in the bottom, [2]. Accordingly, the structure and performance can be used to classify membranes desalination capacity. Figs. 7–11 show that M1, M2, M3, M4 and M5 membranes have an active thin dense top layer, where the thickness of membranes are 230, 200, 90, 109 and 150 μm respectively, the thickness of membranes were measured using digital thickness tester. According to that, these membranes could be classified as RO membrane based on salt rejection percentage. Thus, the performance test of the prepared membranes have been tested to check that.

3.2.2. Mechanical properties

The large-scale blended PVC/CA membranes were fabricated, using the casting machine shown in Fig. 1, for application in pilot scale parallel flat sheet modules or spiral wound modules. Accordingly, mechanical properties of membranes are of high importance and had to be tested. The testing results, Fig. 12, indicate that the membrane M1 has the highest tensile strength and elongation, which were 25.2 kg/cm^2 and 8% respectively. Results show that tensile strength of M5, M2 and M4 were close to each other and close to tensile strength of M1. Tensile strength of M5, M2, and M4 were 24.6, 24.2 and 23.4 kg/cm^2 respectively. M3 ranked the last with only 20 kg/cm^2 . In elongation testing, M1 ranked first with M5, M4 and M2 trailing with close results of 8% 7.5% 7% and 6.7% respectively. Again M3 ranked last with only 4.5%. The results indicate that the higher capacity of the blend membranes to withstand higher feed pressures could be given as M1, M5, M2, M4 and M3, respectively. Although, M4 ranked slightly better than M2 in elongation test, the difference in elongation testing would not overweight the difference in tensile strength favoring M2.

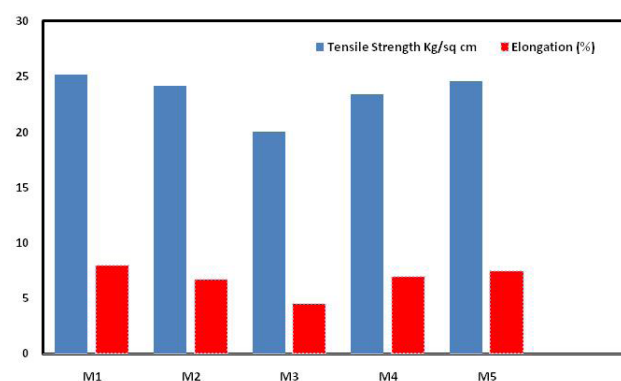


Fig. 12. Mechanical properties of blend membranes PVC/CA (M1–M5).

3.2.3. Membrane porosity and BET area

Porosity and inner surface area of prepared blend membranes were determined and illustrated in Table 2. Results showed that the mean pores diameter of M1 and M5 are close to each other; 6.7 and 6.4 nm. This is attributed to the dense top layer and the asymmetric structure of M1 and M2 membranes. Cellulose acetate as a second polymer plays the main role in the dense top layer formation, where it controls the polymeric solution viscosity. The time of the membrane formation after coagulation step depends on the speed of the de-mixing step of phase separation [16–19]. M2 and M3 have a weight percentage of 1% cellulose acetate (CA) in the polymeric solution, leading to porosity of these membranes to be higher than M1 and M5, due to the decrease in thickness of the dense top layer. However, M4 has high porosity 40.3% compared to M1 and M5 due to having 3% CA in its polymeric mixture, which led to fast de-mixing step during phase separation process. Fast de-mixing led to formation of asymmetric fingers-like pores, which, led to the increase in M4 porosity as shown in membrane SEM section.

3.2.4. Thermo gravimetric analysis (TGA) and differential scanning calorimetry (DSC)

The TGA curves of the prepared membranes PVC without the addition of CA (continuous lines) and blend membrane M5; PVC/CA (dashed lines) are shown in Fig. 13. It has been seen in the literature that the thermal degradation of CA starts at 260°C without any additives [30]. In current study, results in Fig 13 show that combination of CA and PVC provides an increase in thermal stability, as PVC/CA blend membrane shows that thermal degradation starts at 320 C, which is higher than thermal degradation start point of pure CA (260°C) and pure PVC (289°C). The glass transition temperature was measured from DSC curves as shown in Fig. 13 to interpret the structure of membrane during employing a thermal analysis on a membrane. Blend membrane PVC/CA provides the highest glass transition temperature which is 72°C compared to that of pure PVC membrane (65°C). Given that, glass transition temperature of pure CA is reported in literature as 55°C [30]. Higher glass transition temperature means that the membrane has high free volume fraction and more flexible structure [31].

Table 2
Measurement of BET area and pores characterization

Membrane type	BET area m ² /g	Mean pore diameter (nm)	Porosity%
M1	8.03	6.7	30.1
M2	6.2	8.5	34.3
M3	2.55	27.2	45.2
M4	5.7	11.5	40.3
M5	6.7	6.4	29.5

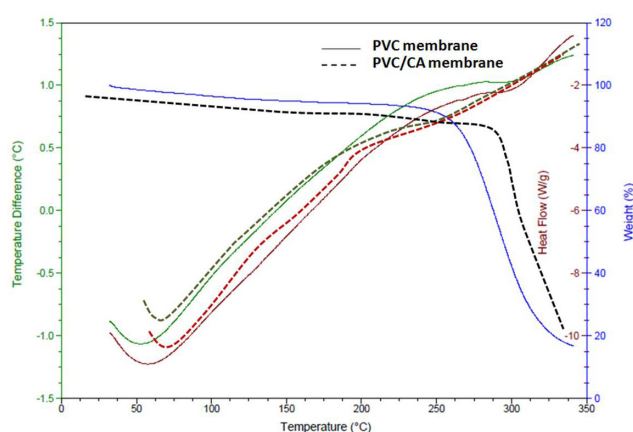


Fig. 13. TGA and DSC measurement for blend PVC/CA membrane and PVC pure membrane.

3.3. Membrane performance measurements

3.3.1. Effect of membrane type on performance

The performance test of the prepared PVC/CA membranes was conducted to classify the fabricated membranes, for which salty water they would be able to desalinate. The test also aimed at ensuring that the produced membranes morphology is free of defects, to ensure its suitability for industrial scale applications. The performance of the fabricated membranes was evaluated and plotted in Figs. 14,15. The results indicate that the addition of CA affects membrane's salt rejection and permeate flux. Results showed that, polymeric solution with 14% PVC and 2% CA produces the membrane with best performance. The addition of CA along with non solvent PEG to the polymeric solution leads to acceleration of the phase separation rate that restricts the aggregated polymers rearrangement and would produce a membrane with dense layer and asymmetric structure [19,30,32].

Figs. 14, 15 show the performance of prepared membranes in terms of salt rejection percentage and permeate flux respectively. The experiments were performed under fixed operating pressure of 30 bars using different salt concentrations (5000, 18000 and 45000 ppm) to determine the desalination capacity of these membranes. Figs. 14, 15 show that the membranes have a high salt rejection starting from 97% up to 99.6%, and a good permeate flux starting from 22 up to 95 L/m²·h. Results showed that that M5 has the best

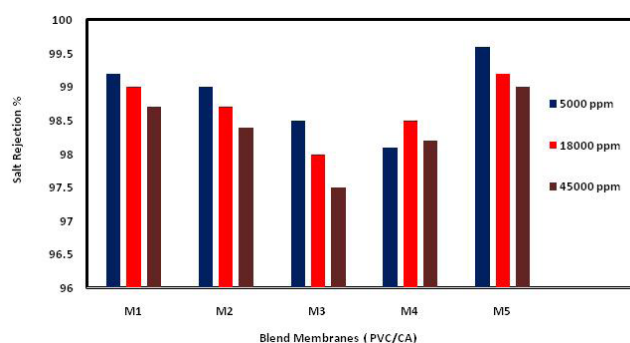


Fig. 14. Salt rejection percentage of blends membranes PVC/CA (M1–M5) at 30 bar.

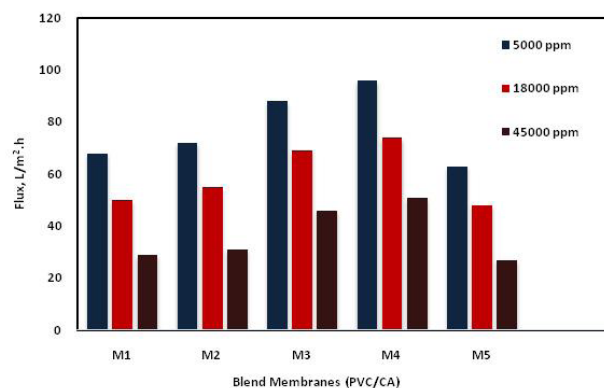


Fig. 15. Permeate flux for of blends membranes PVC/CA (M1–M5) at 30 bar.

salt rejection, and would be suitable for seawater desalination. All membranes proved to be capable of brackish water desalination. Therefore, these membranes can be classified as RO membranes and are suitable for water desalination.

Most prepared polymeric RO membranes in this work and in reviewed works have thickness in the range of 70–200 μm [28–32]. In general, RO membranes should carry pressures up to 80 bars to overcome the osmotic pressure of saline sea water [1–4,28–32]. Accordingly, these membranes must be supported by fabrics or metal porous supports. In our work, we support the prepared membranes by a fine porous stainless-steel support disk during desalination test, as shown in Fig. 2. The membrane samples are sandwiched between two stainless steel screens to enable them to withstand the required high pressures.

3.5. Model verification

The experimental results of salt rejection and permeate flux indicate matching with the FDRSM predicted results, due to increasing the PVC polymer percentage with an appropriate proportion of CA performed reverse osmosis membranes with asymmetric structure. According to the experimental results and FDRSM predicted results, the produced membranes were classified to which kind of salty water it can desalinate. As shown in Table 3, M5 is classified to be suitable for high salinity sea water desalination. M1

Table 3
Classification of produced membranes for water desalination

Membrane	Salty water concentration				
	1000–5000 ppm	5000–10000 ppm	10,000–20,000 ppm	20,000–35,000 ppm	35,000–45000 ppm
M5	✓	✓	✓	✓	✓
M1	✓	✓	✓	✓	
M2	✓	✓	✓		
M4	✓	✓			
M3	✓				

✓ : means the membrane can be used to desalinate water with this salt concentration, while the
■ : means best region for using this membrane.

can be used in sea water and high brackish water desalination. Also, M5 and M1 can be used to desalinate a wide range of salty water concentrations. M2, M4 and M3 can be used to desalinate different grades of brackish water.

The compatibility between PVC with CA was achieved by producing different kinds of blend membranes, where the membranes pores sizes were shifted to small pores size depending on the CA percentage. Moreover, hydrophilicity of the membranes increased with increasing CA content which is attributed to the acetyl group in cellulose acetate chains. Increasing the hydrophilicity of membrane led to improvement in the permeate flux. Also, decreasing the sizes of membrane pores increased membrane's dense top layer and provided high salt rejection [33].

4. Conclusions

PVC/CA blend membranes have been prepared successfully by phase inversion process. The factorial design with response surface methodology (FDRSM) was employed using design experiment software to determine optimum conditions for PVC/CA RO blend membranes preparation. Prepared membranes have been characterized using SEM and by investigating the membranes mechanical properties, the following conclusions can be drawn from the present work:

- The factorial design with response surface methodology results indicated that increasing polymers mixing temperature from 25 to 60°C improved membrane flux and decreased the salt rejection, while increasing the main polymer (A) percentage decreased the flux and improved the salt rejection, which matched with the performance results due to dense top layer of produced membranes.
- SEM results showed that the prepared blend membranes have a dense top layer and an intermediate spongy like structure whereas the bottom layer is highly porous. SEM images illuminate a good interaction between PVC and CA.
- M1 membrane showed the best mechanical properties compared to other prepared membranes, with a tensile strength of 27 kg/cm² and 10% elongation. It also has ranked the second in salt rejection capacity.

- The performance test of prepared membranes was carried out using various salt concentration, the results show that membrane M5 (PVC 14% and CA 2%) provides highest salt rejection. Also, it has ranked the second in mechanical properties test. Accordingly, membrane M5 can be used in seawater desalination, while other membranes can be used in brackish water desalination.

References

- G. Kang, Y. Cao, Development of antifouling reverse osmosis membranes for water treatment: A review, *Water Res.*, 46 (2012) 584–600.
- L. Yu, K. Deana, L. Lin, Polymer blends and composites from renewable resources, *Prog. Polym. Sci.*, 31 (2006) 576–602.
- A. EL-Gendi, A. Deratani, S.A. Ahmed, S. Ali, The development of polymeric membrane via casting technology for water desalting, *Procedia Eng.*, 44 (2012) 1772.
- M. Gamal Khedr, Development of reverse osmosis desalination membranes composition and configuration: future prospects, *Desalination*, 153 (2002) 295–304.
- S. Ehsan, M. Toraj, Cellulose acetate (CA)/polyvinylpyrrolidone (PVP) blend asymmetric membranes: Preparation, morphology and performance, *Desalination*, 249 (2009) 850–854.
- C. Yun, X. Peng, X. Yang, G. Zhang, L.N. Lei, S. Land, L. Hui, Characterization of regenerated cellulose membranes hydrolyzed from cellulose acetate, *Chinese J. Polym. Sci.*, 20(4) (2002) 379–375.
- M. Sivakumar, D. Mohana, R. Rangarajan, Studies on cellulose acetate-polysulfone ultrafiltration membranes II. Effect of additive concentration, *J. Membr. Sci.*, 268 (2006) 208–219.
- G. Arthanareeswaran, S.K. Ananda, Effect of additives concentration on performance of cellulose acetate and polyethersulfone blend membranes, *J. Porous. Mater.*, 17 (2010) 515–522.
- R. Mahendran, R. Malaisamy, D. Mohan, Preparation, characterization and effect of annealing on performance of cellulose acetate/sulfonated polysulfone and cellulose acetate/epoxy resin blend UF membranes, *Eur. Polym. J.*, 40 (2004) 623–633.
- A. EL-Gendi, A. Deratani, S.A. Ahmed, S. Ali, Development of polyamide-6/chitosan membranes for desalination, *Egypt J. Petrol.*, 23 (2014) 169–173.
- H. Abdallah, M.S. Shalaby, A.M.H. Shaban, Performance and characterization for blend membrane of PES with manganese(III) acetylacetonate as metalorganic nanoparticles, *Int. J. Chem. Eng.*, 2015 (2015) 1–9.
- M. Shaban, H. Hamdy, H. AbdAllah, L. Said, A. Abdel Khalek, Effects of TiO₂ NTs% on polyethersulfone/TiO₂ NTs membranes, *J. Mater. Sci. Eng. A*, 5(1–2) (2015) 65–68.

- [13] H. Abdallah, A.F. Moustafa, A.A. Anezi, H.E.M. El-Sayed, Performance of a newly developed titanium oxide nanotubes/polyethersulfone blend membrane for water desalination using vacuum membrane distillation, *Desalination*, 346 (2014) 30–36.
- [14] S.S. Ali, H. Abdallah, development of PES/CA blend RO membrane for water desalination, *I.RE.C.H.E.*, 4 (2012) 316–323.
- [15] H. Abdallah, S.S. Ali, Thermodynamic modeling of PES/CA blend membrane preparation, *I.RE.C.H.E.*, 4 (2012) 455–465.
- [16] M. Frommer, R. Messalam, Mechanism of membrane formation. VI. Convective flows and large void formation during membrane precipitation, *Ind. Eng. Chem., Prod. Res. Dev.*, 12 (1973) 328–333.
- [17] N. Ghaemi, S.S. Madaeni, A. Alizadeh, P. Daraei, V. Vatanpour, M. Falsafi, Fabrication of cellulose acetate/sodium dodecyl sulfate nanofiltration membrane: Characterization and performance in rejection of pesticides, *Desalination*, 290 (2012) 99–106.
- [18] K. Wa, D. Leea, P. K. Chanb, X. Feng, Morphology development and characterization of the phase-separated structure resulting from the thermal-induced phase separation phenomenon in polymer solutions under a temperature gradient, *Chem. Eng. Sci.*, 59 (2004) 1491–1504.
- [19] T.D. Kusworo, Budiyo, A.I. Wibowo, G.D. Harjanto, A.D. Yudisthira, F.B. Iswanto, Cellulose acetate membrane with improved perm-selectivity through modification dope composition and solvent evaporation for water softening, *Res. J. Appl. Sci. Eng. Technol.*, 7(18) (2014) 3852–3859.
- [20] X. Zhang, Y. Chen, A. Konsowa, X. Zhu, J.C. Crittenden, Evaluation of an innovative polyvinyl chloride (PVC) ultrafiltration membrane for wastewater treatment, *Sep. Purif. Technol.*, 70 (2009) 71–78.
- [21] B. Liu, C. Chen, W. Zhang, J. Crittenden, Y. Chen, Low-cost antifouling PVC ultrafiltration membrane fabrication with Pluronic F 127: effect of additives on properties and performance, *Desalination*, 307 (2012) 26–33.
- [22] A. Alkudhiri, N. Darwish, N. Hilal, Membrane distillation: a comprehensive review, *Desalination*, 287 (2012) 2–18.
- [23] S. Pacharasakoolchai, W. Chinpa, Improved permeation performance and fouling-resistance of poly(vinyl chloride)/polycarbonate blend membrane with added Pluronic F127, *Songklanakarin J. Sci. Technol.*, 21036(2) (2014) 209–215.
- [24] Y. Zhao, J. Lu, X. Liu, Y. Wang, J. Lin, N. Peng, J. Li, F. Zhao, Performance enhancement of polyvinyl chloride ultrafiltration membrane modified with graphene oxide, *J. Colloid. Interface Sci.*, 480 (2016) 1–8.
- [25] Z. Yu, Y. Zhao, B. Gao, X. Liu, L. Jia, F. Zhao, Performance of novel a Ag-n-TiO₂/PVC reinforced hollow fiber membrane applied in water purification: in situ antibacterial properties and resistance to biofouling, *RSC Adv.*, 5 (2015) 97320–97329.
- [26] S. Mei, C. Xiao, X. Hu, Preparation of porous PVC membrane via a phase inversion method from PVC/DMAc/water/additives, *J. Appl. Polym. Sci.*, 120 (2011) 557–562.
- [27] J.M. Arsuaga, A. Sotto, G. del Rosario, A. Martínez, S. Molina, S.B. Teli, J. de Abajo, Influence of the type, size, and distribution of metal oxide particles on the properties of nanocomposite ultrafiltration membranes, *J. Membr. Sci.*, 428 (2013) 131–141.
- [28] B.K. Pramanik, Y. Gao, L. Fan, Felicity A. Roddick, Z. Liu, Antiscalting effect of polyaspartic acid and its derivative for RO membranes used for saline wastewater and brackish water desalination, *Desalination*, 404 (2017) 224–229.
- [29] K. Yamamoto, S. Koge, T. Gunji, M. Kanezashi, T. Tsuru, J. Ohshita, Preparation of POSS-derived robust RO membranes for water desalination, *Desalination*, 404 (2017) 322–327.
- [30] G. Arthanareeswaran, P. Thanikaivelan, K. Srinivasn, D. Mohan, M. Rajendran, Synthesis, characterization and thermal studies on cellulose acetate membranes with additive, *Eur. Polym. J.*, 40 (2004) 2153–2159.
- [31] H.A. Shnawa, M.N. Khalaf, Y. Jahani, A.H. Taobi, Efficient thermal stabilization of polyvinyl chloride with tannin-Ca complex as bio-based thermal stabilizer, *Mater. Sci. Appl.*, 6 (2015) 360–372.
- [32] A. El-Gendi, H. Abdallah, A. Amin, S.K. Amin, Investigation of polyvinylchloride and cellulose acetate blend membranes for desalination, *J. Mol. Struct.*, 1146 (2017) 14–22.
- [33] A. Behboudi, Y. Jafarzadeh, R. Yegani, Polyvinyl chloride/polycarbonate blend ultrafiltration membranes for water treatment, *J. Membr. Sci.*, 534 (2017) 18–24.